

Bank stability analysis for regime models of vegetated gravel bed rivers

Brett C. Eaton*

Department of Geography, The University of British Columbia, Vancouver, British Columbia, Canada

*Correspondence to:
Brett C. Eaton, Department
of Geography, The University
of British Columbia, Vancouver,
British Columbia, Canada V6T
1Z2. E-mail: brett.eaton@ubc.ca

Abstract

A new bank stability analysis procedure is developed for use in rational regime models predicting reach average channel dimensions. The performance of a regime model using this new bank stability formulation is compared against that for a model using the modified friction angle approach proposed by Millar and Quick (1993). The bank stability assessment is based on a conceptual model that more closely represents conditions found in gravel bed rivers with vegetated floodplains: the primary effect of vegetation is its contribution to a stable upper bank, the position of which is determined by erosion of unvegetated bed material at the toe of the bank. The vertical height of the upper bank is estimated using a simple slab failure model and assigning an effective cohesion to the vegetation-reinforced soil. The geometry of the lower slope and the width of the channel are determined iteratively using the regime approach described by Eaton *et al.* (2004). A comparison of the predicted stream channel widths for stable gravel bed channels classified according to riparian vegetation type (Hey and Thorne, 1986) showed that this new formulation increases model accuracy, especially for the more densely vegetated channel types. Since the strength parameters used in the model can be estimated from the observed bank geometry, the potential for applying and testing rational regime models in the field has been significantly improved. Copyright © 2006 John Wiley & Sons, Ltd.

Keywords: bank stability; regime theory; riparian vegetation; gravel bed rivers

Received 1 November 2005;
Revised 22 January 2006;
Accepted 9 February 2006

Introduction

Rational regime models explicitly represent the relations between the driving variables of sediment supply and stream discharge, boundary conditions such as bank erodibility and bed surface texture, and channel morphology. They predict the average reach-scale channel dimensions, and are most usefully interpreted as physically based models of downstream hydraulic geometry and as frameworks for evaluating potential reach-scale channel response to changes in either the driving variables or the boundary conditions.

Tests of the regime theory formulation presented by Eaton *et al.* (2004) reveal that, if a bank stability analysis is used to constrain the model, the dimensions of channels developed in the laboratory can be fairly accurately predicted (Eaton *et al.*, 2004; Eaton and Millar, 2004). Similarly, the reach-average dimensions of channels in the field where the banks are only slightly influenced by vegetation can be relatively accurately modelled. However, as the vegetation becomes successively more dense, the model fares progressively less well, and a significant scale effect not incorporated into the standard regime model formulation presents itself (Eaton and Millar, 2004).

By way of analogy with the infinite slope model used to assess hillslope stability, channel bank strength can be divided into two components. The first represents the frictional properties of the material, which relates the critical shear stress required for entrainment of the bank material to the normal force acting on the bank, which, in the case of bank stability in response to a shearing flow is simply the mass of the characteristic bank grain size. This frictional property is expressed as a friction angle, ϕ , and is dimensionless in the sense that it relates the critical dimensionless shear stress for a channel bank to the average bank angle and the critical Shields number. The second component is the effective cohesion, which may be attributable to true cohesive forces, matric suction within the unsaturated part of the

bank and/or root reinforcement from riparian vegetation. This contribution is not dimensionless, since the magnitude of the force is strongly related to the scale of the vegetation (i.e. its rooting depth and rooting density) and the scale of the grain size – cohesion only occurring as it does in only the finest size fractions. In any case, the magnitude of the cohesive forces must be expressed in the dimensional units of shear strength (usually kilopascals).

For the sake of simplicity, bank strength in the model presented by Eaton *et al.* (2004) is expressed using an apparent friction angle, ϕ' , that represents bank strength using only a single parameter: this is tantamount to assuming that all bank strength is attributable to the frictional properties of the bank material alone. Effectively, then, bank erodibility is expressed relative to bed erodibility and, as a result, absolute bank strength scales with the channel dimensions (Eaton *et al.*, 2004; Millar, 2005). While this is convenient when representing the underlying physical relations in dimensionless form, it becomes less convenient when dealing with real, scale dependent phenomena such as alluvial channels with bank vegetation that does not scale with channel dimensions. Furthermore, it is difficult to assign physical meaning to or define a measurable surrogate for ϕ' . As a consequence, it has not yet been reliably calibrated in the field for bank strengths greater than the natural friction angle, ϕ , where we know that all of the bank strength is attributable to the frictional properties alone.

In this paper, a modified bank stability analysis is presented that attempts to make use of both the frictional strength parameter and the scale-dependent cohesive strength parameter. We have applied this model to the alluvial channels described by Hey and Thorne (1986). It is assumed that their channels exhibit a cohesionless lower bank and a cohesive or vegetation-modified upper bank, typical of gravel bed streams. This situation arises in the field as a direct consequence of the way in which sediment is transported and sequestered in alluvial systems: the cohesionless lower bank unit is the product of bedload deposition and storage in channel bars, while the upper bank section is the product of bar top and overbank deposition of finer (possibly cohesive) sediments, combined with vegetal colonization. Therefore, this model is most likely generally applicable to the reach-scale characterization of most streams with a distinct bedload/suspended load floodplain stratigraphy.

While this approach to bank stability loses some of the natural appeal of the simpler, scale independent ϕ' , it is based on an assumed geometry that is similar to that observed in the field, and the bank strength-related parameters may well be more easily calibrated based on field observations.

The Model

A properly constrained model for predicting channel dimensions must consider the effect of bank strength on stream channel dimensions (Millar and Quick, 1993; Griffiths and Carson, 2000), or else the predicted channel dimensions will inevitably exceed the observed dimensions (Eaton and Millar, 2004) for all but the most erosion-resistant channel banks. The regime model described by Millar and Quick (1993) and Eaton *et al.* (2004) uses a trapezoidal channel geometry that comprises the bottom width (P_{bed}), channel depth (Y_o), side slope angle (θ) and average channel slope (S). The bed and banks are assumed to have a characteristic grain size (D). The geometry is varied iteratively so as to determine the channel configuration with the highest system-scale flow resistance (Eaton *et al.*, 2004), which corresponds to the most stable and hence most probable channel state (cf. Huang *et al.*, 2004). If surface grain size and bedform roughness are constant, then this flow resistance maximization is achieved by minimizing the channel slope (Chang, 1979), subject to the ability of the channel to transport the imposed sediment supply with the available stream discharge, which is equivalent to maximizing the transport capacity of the stream for a constant slope (White *et al.*, 1982). Stream table experiments suggest that this sort of slope-dominated channel response does indeed occur when the stream banks are relatively erodible (Eaton and Church, 2004). The bank stability equations are presented by Millar and Quick (1993) and in an appendix to Eaton *et al.* (2004) available online.

The bank stability analysis presented in this paper arises from the observation that stream banks seldom exhibit a simple linear profile. Rather, stream banks in gravel bed rivers tend to exhibit a vertical upper section, composed in large part of overbank deposits, that is influenced by the cohesion of the fine grained sediment found there and/or the binding effect of root structures (Figure 1). The lower part of the bank, originally deposited in channel bars, is typically composed of cohesionless material with a grain size distribution similar to the bed material found in the channel, and is not usually affected by the root structure above. It is proposed that fluvial erosion of the cohesionless lower bank is primarily responsible for determining the bank position and the average channel width, while the cohesive upper bank persists only where it is not undercut by fluvial erosion at the toe.

The modification proposed herein involves changing the assumed channel geometry and recasting the bank strength analysis in terms of an effective cohesion (C') characteristic of the upper channel bank and a friction angle (ϕ) characteristic of the cohesionless lower bank, which is assumed to have a characteristic grain size similar to the channel bed (cf. Figure 1). The modified bank geometry is shown in Figure 2. On the left side of the diagram, the

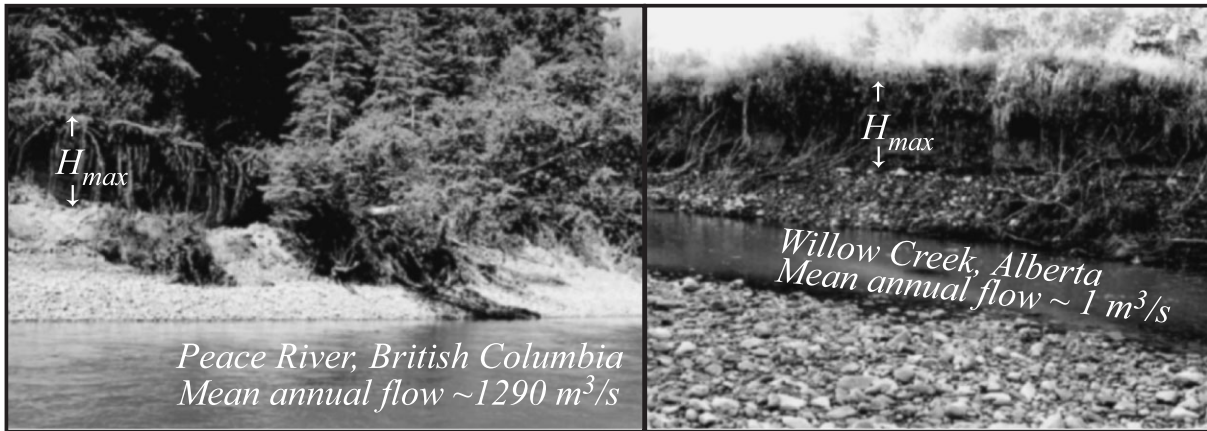


Figure 1. Examples of typical stream banks in gravel bed stream channels influenced by vegetation. Note the signs of mass failure of the upper vertical bank and the linear, low angle lower bank in both examples.

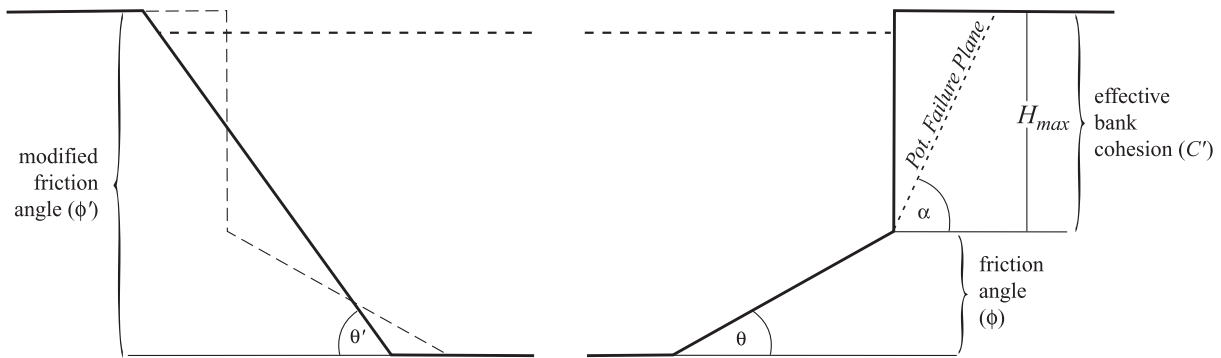


Figure 2. Assumed channel bank geometry employed by the regime models using a modified friction angle (ϕ') formulation (shown at the left bank), and a composite bank stability analysis based on an effective cohesion (C') and friction angle (ϕ) (right bank). The geometric relation between the two formulations has been indicated by overlaying the composite bank profile as a dashed line on the left panel.

original formulation using ϕ' is presented for comparison. On the right hand side, the modified bank configuration is presented.

It is assumed that the upper bank is vertical with a reach-average height that is proportional to the effective cohesive strength of the upper bank material. It is also assumed that the failure mode for the upper bank is adequately described by a simple slab failure stability analysis, such as that used by Istanbulluoglu *et al.* (2005). Various researchers have adapted this general approach to modelling bank stability in streams where the bank is entirely cohesive (Darby and Thorne, 1996; Darby *et al.*, 2000) and slab failures appear to be relatively common in this kind of stream (Dapporto *et al.*, 2003). Here, a slab failure model is used to predict the maximum stable height of a vertical bank based on an apparent cohesion value for the bank material. Istanbulluoglu *et al.* (2005) present an equation for predicting the critically stable height (H_{max}) in the absence of tension cracks for a dry soil. Their equation is

$$H_{max} = \frac{2C'}{\gamma_b \cos \alpha} \left[\frac{1}{\sin \alpha - \cos \alpha \tan \phi} \right] \tag{1}$$

where α is the angle of the potential slab failure plane ($\alpha = 45 + \phi/2$, following Carson and Kirkby (1972, p. 116)) and γ_b is the bulk unit weight of the bank material. This represents an upper bound to the stable bank height, since the development of significant pore pressures will reduce H_{max} . Assuming a fully saturated channel bank with a hydrostatic

pore pressure distribution, one can develop an expression that represents the lower bound for H_{\max} . The equation (after Istanbulluoglu *et al.*, 2005) is

$$H_{\max} = \frac{2C'}{\gamma_b \cos \alpha} \left[\frac{1}{\sin \alpha - (\cos \alpha - \gamma/\gamma_b) \tan \phi} \right] \quad (2)$$

where γ is the unit weight of water. Since the intent here is not to perform a slab stability analysis but merely to relate the vertical height for the upper bank in the regime model geometry to the effective cohesion, Equations (1) and (2) are used to specify a reasonable range of effective cohesion values. Actual bank failure events will be influenced by the development of pore water pressure distributions possibly quite different from hydrostatic (Rinaldi and Casagli, 1999; Simon *et al.*, 1999), the development of tension cracks intercepting the potential failure plane (Darby and Thorne, 1996) and the specific arrangement of individual plants and root systems upon and within the bank (Abernethy and Rutherford, 2000). The regime model is formulated at a scale that averages out these details, thus making a complete and physically accurate slab stability analysis impractical and unnecessary for the purposes of predicting reach average channel dimensions.

Analysis of the stability of the lower bank proceeds in the normal way, as described by Millar and Quick (1993). The shear stress acting on the bank is estimated using the empirical functions developed by Flinham and Carling (1988), and the critical shear stress for bank erosion (τ_{cb}) is determined based on the Shield number (τ_c^*) and the bank angle:

$$\tau_{cb} = \tau_c^*(\gamma_s - \gamma)D \sqrt{1 - \frac{\sin^2 \theta}{\sin^2 \phi}} \quad (3)$$

The parameters γ_s and σ represent the unit weights of the sediment grains and water, respectively. The advantage of this approach is that the bank angle (θ) calculated by the model is equivalent to the average angle of the lower banks in the field (i.e. the angle of the banks shown in Figure 1), and thus comparisons between field measurements and model predictions of θ should give a reasonable measure of model performance. Furthermore, bank strength can potentially be parametrized in the field by measuring the average height of the vertical bank sections. In contrast, the ϕ' approach accounts for increased bank strength (due to vegetation, in particular) by increasing the angle of frictional resistance, and thus calculates an apparent bank angle (θ') that has no obvious analogue in the field. It is unclear how one might parametrize ϕ' based on simple field observations.

While setting the upper bank section height equal to H_{\max} is only a conceptual inclusion of slab stability analysis, it represents an improved parametrization of the effect of cohesion and root structure on bank strength and it is consistent with the relatively large spatial and temporal scales at which regime concepts apply. In the field, it may well be that the average upper bank height is somewhat less than the critical height, which will introduce a tendency to overestimate the effective bank cohesion using Equations (1) and (2). The magnitude of this potential bias remains to be assessed in the field, but the preliminary tests that follow suggest that this potential bias has, at worst, only a modest effect.

Preliminary Tests

In order to test this new model, the analysis of the data of Hey and Thorne (1986) presented by Eaton and Millar (2004) was repeated using this refined bank stability analysis. The regime model was used to calculate the channel widths for the stable gravel bed stream channels reported by Hey and Thorne (1986). A single upper bank height value was assigned to each of the four vegetation classes of Hey and Thorne, and related to the inferred effective bank cohesion using Equations (1) and (2). The riparian vegetation classes are described as follows: *type I*, grass with no trees or shrubs; *type II*, 1–5 per cent shrubs and trees; *type III* 5–50 per cent shrubs and trees; *type IV*, more than 50 per cent trees and shrubs. The value of H_{\max} for each vegetation class was varied to produce the best average fit to the field data of Hey and Thorne (Table I).

For type IV channels, the upper bank height that produced the best fit was greater than the observed channel depth for the smallest four channels in the dataset, and the model was unable to converge on a solution. These data are excluded from the analysis. It is possible that in these smallest channels the effect of vegetation extends below the channel toe, producing banks that are not conceptually similar to Figure 2, in which case the model would not be

Table I. Strength parameters, bank angles and normalized standard error¹ for predicted channel widths for both regime model formulations

C' model	H_{max} (m)	Mean θ (°)	Std Dev.(θ) (°)	Norm. SE¹
Type I	0.36	16.1	3.7	0.315
Type II	0.53	16.2	3.1	0.166
Type III	0.89	17.8	3.5	0.182
Type IV	1.07	18.1	2.9	0.203
All data	–	17.1	3.3	0.214

ϕ' Model	ϕ' (°)	Mean θ' (°)	Std Dev.(θ') (°)	Norm. SE¹
Type I	40	21.2	4.6	0.307
Type II	45	24.8	4.4	0.231
Type III	49	29.5	6.1	0.402
Type IV	50	35.3	7.5	0.471
All data	–	27.9	7.9	0.338

¹ Calculated by $(1/df)\sum \sqrt{(1 - W_{est}/W_{obs})^2}$; W_{est} and W_{obs} are the estimated and observed widths; df is the degrees of freedom.

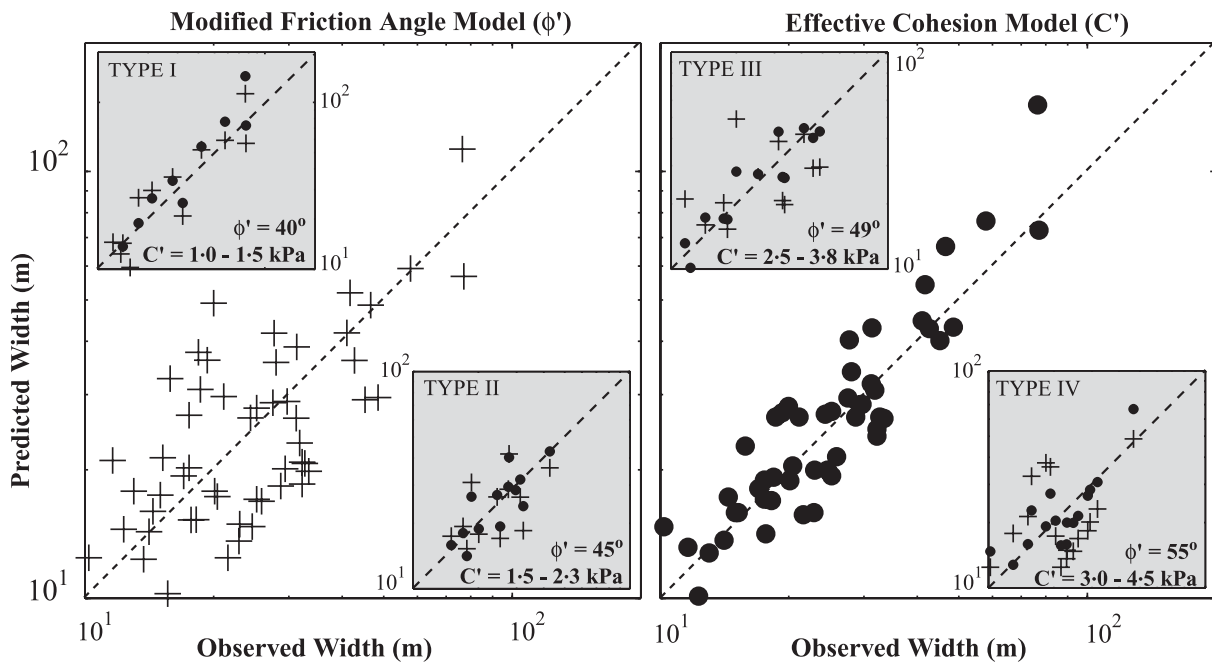


Figure 3. Observed and predicted widths for the dataset of Hey and Thorne using a regime model representing bank strength as a modified friction angle (left panel), and a regime model representing bank strength as an effective cohesion and a friction angle of 30° (right panel). The data are also presented by vegetation type in the inset panels (using + for the ϕ' model and solid circles for the C' model).

appropriate. It may also be that the water table in these smallest streams limits the rooting depth and/or affects the species composition, in which case the upper bank dimensions should vary systematically with channel depth. In either case, not enough information is available to appropriately model these channels.

Figure 3 presents a comparison of the predicted widths for the bank stability analysis reported by Eaton and Millar (2004) and for the bank stability analysis presented here. The range of C' values for each vegetation type are presented in the figure, along with the ϕ' values from Eaton and Millar (2004). The model fit is visibly improved for the dataset

as a whole. The normalized standard error associated with the two model formulations was estimated for the dataset as a whole and for each vegetation class (Table I). The overall error is reduced from 33.8 per cent of the observed width for the ϕ' model to 21.4 per cent for the C' model. The largest improvements occur for the most densely vegetated channels (types III and IV), where the error for the C' model is about half that for the ϕ' model. It is worth noting that, whereas ϕ' model performance declines with increasing vegetation density, the revised model formulation presented here seems to perform about equally well for all vegetation types, and it predicts lower bank angles that are similar for all vegetation types (Table I).

In fact, the type I channels are least well predicted by the C' regime model. A significant component of the total error for type I channels is attributable to a single stream channel (the largest in the dataset of Hey and Thorne with a formative discharge of $424 \text{ m}^3 \text{ s}^{-1}$) for which the predicted width is almost twice the observed width: when this data point is removed from the dataset, the normalized standard error falls to 26 per cent. The smallest type I channels are also poorly described by the model, having widths systematically larger than predicted. If the channels with formative discharges less than $9 \text{ m}^3 \text{ s}^{-1}$ are excluded from the dataset, the standard error falls to 21 per cent, in line with the standard errors for the other vegetation types. The reasons for these deviations at either end of the discharge distribution are not clear, but may be related to the rooting patterns for grass, which, unlike trees and shrubs, typically forms dense, vertically oriented roots in only the upper part of the soil. As a result, banks dominated by grasses may tend to fail by other mechanisms than slab failure, such as cantilever or block type failures, an effect that may well introduce the deviations at either end of the channel scale distribution. The observed scale effects may also be attributable to systematic differences in the vegetation species, and/or the distribution of these species within the channel boundaries (e.g. whether the bank surface is vegetated or not). These deviations may also be related to the nature of the overbank sediments, which would tend to be coarser and less cohesive for the smaller basins, and finer and more cohesive for the largest basins.

It is also informative to compare the 'best' values of C' for each vegetation type with the data to other reported effective cohesion values, based on vegetation type. If we assume that most of the sediment deposited on the floodplains of the channels of Hey and Thorne is not cohesive and that the effective cohesion due to soil moisture tension is negligible at failure, then root cohesion must be the dominant component of C' . The ranges of C' values estimated for types I, II, III and IV are 1.0–1.5, 1.5–2.3, 2.5–3.8 and 3.0–4.5 kPa, respectively. These are *average* values for the entire soil profile. They do not take into account the covariation of C' with root density within the bank. For example, due to the particularly high density of grass root masses, C' in the uppermost parts of the bank for a type I channel may be much higher than for the other vegetation classes, reaching values as high as 13 kPa (Pollen and Simon, 2005) to 18 kPa (Simon and Collison, 2002). However, grass roots tend to be concentrated in the upper part of the soil profile, so the average cohesion, which is the appropriate one for this sort of reach-scale analysis, is actually lower than it is for the other vegetation types.

In an examination of debris slides in the Pacific Northwest, Buchanan and Savigny (1990) estimated depth-averaged root cohesion (C_r) directly by reconstructing the conditions at failure for nine different events. Their values range from about 1.6 for the least dense vegetation type (group I, which Buchanan and Savigny describe as 'understorey') to just under 3.0 kPa for a second growth forest (group III). Old growth forests in the study area of Buchanan and Savigny did not experience any failures, but one previous study (Swanston, 1970) suggests that undisturbed forests may have root cohesion values between 3.4 and 4.4 kPa, while another (Burroughs and Thomas, 1977) suggests that root cohesion values for old growth can be as high as 8.9 to 16.7 kPa. It is evident that the range of effective cohesion determined from the best-fit H_{\max} values predicted by the regime model are of the appropriate order of magnitude, and the values for each class roughly correspond to the values determined for similar vegetation classes in a more complete slope stability analysis (Buchanan and Savigny, 1990). This suggests that assuming the upper bank height is equal to H_{\max} introduces at worst only a modest potential bias in the estimated effective cohesion.

Conclusions

The proposed modification to the bank stability analysis included in the rational regime model described by Millar and Quick (1993) and Eaton *et al.* (2004) adds an additional parameter, thus slightly increasing the model complexity. However, since both bank parameters in the new stability analysis can be given unambiguous physical interpretations and directly related to observable conditions in the field, the addition of one more variable seems to be warranted.

Initial tests of this approach suggest that it captures the underlying physics of bank stability relatively well, at least at the reach scale. However, these tests are necessarily predicated on assumptions about the cross sectional shape of the streams being modelled. While these assumptions seem to be reasonable, based on comparing the inferred

effective cohesion with the root cohesion reported in other studies for similar vegetation cover, it may no longer be necessary to resort to them, since the relevant cross sectional parameters (i.e. H_{\max} and θ) can at least potentially be related to measurable quantities in the field. In contrast, the physical manifestation of ϕ' and the corresponding apparent bank angle (θ') are not easily related to channel geometry in the field.

In conclusion, this revised bank strength formulation presents fluvial geomorphologists with the opportunity to more directly test the applicability of regime theory to stream channels that are strongly influenced by riparian vegetation. It is in order to encourage such rigorous testing of this potentially useful tool that this model refinement has been presented, and this is certainly a research direction the author and his colleagues are actively pursuing.

References

- Abernethy B, Rutherford ID. 2000. The effect of riparian tree roots on the mass-stability of riverbanks. *Earth Surface Processes and Landforms* **25**: 921–937.
- Buchanan P, Savigny KW. 1990. Factors controlling debris avalanche initiation. *Canadian Geotechnical Journal* **27**(5): 659–675.
- Burroughs ER, Thomas BR. 1977. *Declining Root Strength in Douglas-Fir After Felling as a Factor in Slope Stability*, U.S. Forest Service Research Paper INT-190. Department of Agriculture: Ogden, UT.
- Carson MA, Kirkby MJ. 1972. *Hillslope Form and Process*. Cambridge University Press: London.
- Chang HH. 1979. Minimum stream power and river channel patterns. *Journal of Hydrology* **41**: 303–327.
- Dapporto S, Rinaldi M, Casagli N, Vannocci P. 2003. Mechanisms of riverbank failure along the Arno River, central Italy. *Earth Surface Processes and Landforms* **28**(12): 1303–1323.
- Darby SE, Gessler D, Thorne CR. 2000. Computer program for stability analysis of steep, cohesive riverbanks. *Earth Surface Processes and Landforms* **25**(2): 175–190.
- Darby SE, Thorne CR. 1996. Development and testing of riverbank-stability analysis. *Journal of Hydraulic Engineering – ASCE* **122**(8): 443–454.
- Eaton BC, Church M. 2004. A graded stream response relation for bedload dominated streams. *Journal of Geophysical Research – Earth Surface* **109**(F03011): doi: 10.1029/2003JF000062.
- Eaton BC, Church M, Millar RG. 2004. Rational regime model of alluvial channel morphology and response. *Earth Surface Processes and Landforms* **29**(4): 511–529.
- Eaton BC, Millar RG. 2004. Optimal alluvial channel width under a bank stability constraint. *Geomorphology* **62**: 35–45.
- Flintham TP, Carling PA. 1988. The prediction of mean bed and wall boundary shear in uniform and compositely roughened channels. *International Conference On River Regime*, White WR (ed.). Wiley: Chichester; 267–287.
- Griffiths GA, Carson MA. 2000. Channel width for maximum bedload transport capacity in gravel-bed rivers, South island, New Zealand. *Journal of Hydrology (NZ)* **39**(2): 107–126.
- Hey RD, Thorne CR. 1986. Stable channels with mobile gravel beds. *Journal of the Hydraulics Division–ASCE* **112**(8): 671–689.
- Huang HQ, Chang HH, Nanson GC. 2004. Minimum energy as the general form of critical flow and maximum flow efficiency and for explaining variations in river channel pattern. *Water Resources Research* **40**(W04502): doi: 10.1029/2003WR002539.
- Istanbuluoglu E, Bras RL, Flores-Cervantes H, Tucker GE. 2005. Implications of bank failures and fluvial erosion for gully development: field observations and modeling. *Journal of Geophysical Research – Earth Surface* **110**(F1): doi:10.1029/2004JF000145.
- Millar RG. 2005. Theoretical regime equations for mobile gravel-bed rivers with stable banks. *Geomorphology* **64**: 207–220.
- Millar RG, Quick MC. 1993. Effect of bank stability on geometry of gravel rivers. *Journal of Hydraulic Engineering – ASCE* **119**(12): 1343–1363.
- Pollen N, Simon A. 2005. Estimating the mechanical effects of riparian vegetation on stream bank stability using a fiber bundle model. *Water Resources Research* **41**(W07025): doi: 10.1029/2004WR003801.
- Rinaldi M, Casagli N. 1999. Stability of streambanks formed in partially saturated soils and effects of negative pore water pressures: the Sieve River (Italy). *Geomorphology* **26**(4): 253–277.
- Simon A, Collison AJC. 2002. Quantifying the mechanical and hydrologic effects of riparian vegetation on streambank stability. *Earth Surface Processes and Landforms* **27**(5): 527–546.
- Simon A, Curini A, Darby SE, Langendoen EJ. 1999. Streambank mechanics and the role of bank and near-bank processes in incised channels. In *Incised River Channels*, Darby SE, Simon A (eds). Wiley: Chichester; 123–152.
- Swanston DN. 1970. *Mechanics of Debris Avalanching in Shallow Till Soils of Southeast Alaska*, US Forest Service Research Paper PNW-103. Department of Agriculture: Portland, OR.
- White WR, Bettess R, Paris E. 1982. Analytical approach to river regime. *Journal of the Hydraulics Division – ASCE* **108**(HY10): 1179–1193.